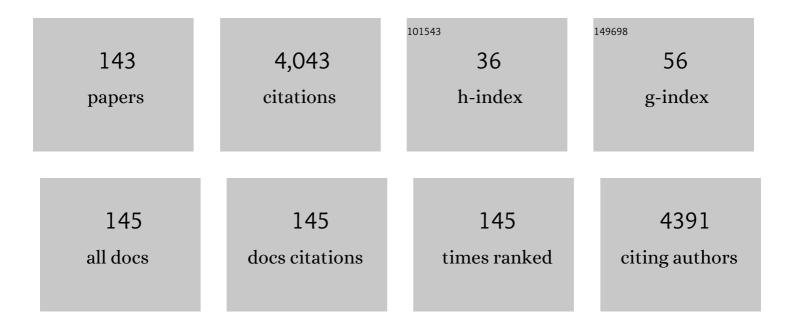
List of Publications by Year in descending order

Source: https://exaly.com/author-pdf/2874177/publications.pdf Version: 2024-02-01



#	Article	IF	CITATIONS
1	Rational confinement engineering of <scp>MOF</scp> â€derived carbonâ€based electrocatalysts toward <scp>CO₂</scp> reduction and <scp>O₂</scp> reduction reactions. InformaÄnÃ-Materiály, 2022, 4, .	17.3	58
2	Boosting selective C2H2/CH4, C2H4/CH4 and CO2/CH4 adsorption performance via 1,2,3-triazole functionalized triazine-based porous organic polymers. Chinese Journal of Chemical Engineering, 2022, 42, 64-72.	3.5	6
3	Facile activation of lithium slag for the hydrothermal synthesis of zeolite A with commercial quality and high removal efficiency for the isotope of radioactive ⁹⁰ Sr. Inorganic Chemistry Frontiers, 2022, 9, 468-477.	6.0	12
4	Interfacial polarization in ultra-small Co3S4â î MoS2 heterostructure for efficient electrocatalytic hydrogen evolution reaction. Applied Materials Today, 2022, 26, 101311.	4.3	21
5	Controllable synthesis of platinum–tin intermetallic nanoparticles with high electrocatalytic performance for ethanol oxidation. Inorganic Chemistry Frontiers, 2022, 9, 1143-1151.	6.0	5
6	Synthesis of P-doped NiS as an electrode material for supercapacitors with enhanced rate capability and cycling stability. New Journal of Chemistry, 2022, 46, 6461-6469.	2.8	5
7	Concave Pt–Zn Nanocubes with Highâ€Index Faceted Pt Skin as Highly Efficient Oxygen Reduction Catalyst. Advanced Science, 2022, 9, e2200147.	11.2	25
8	Enhancing the Stability of the Resin–Dentin Bonding Interface with Ag ⁺ - and Zn ²⁺ -Exchanged Zeolite A. ACS Biomaterials Science and Engineering, 2022, 8, 1717-1725.	5.2	3
9	Low-energy adsorptive separation by zeolites. National Science Review, 2022, 9, .	9.5	41
10	Synthesis of Pure Silica Zeolites. Chemical Research in Chinese Universities, 2022, 38, 9-17.	2.6	6
11	Achieving ultra-dispersed 1T-Co-MoS ₂ @HMCS <i>via</i> space-confined engineering for highly efficient hydrogen evolution in the universal pH range. Inorganic Chemistry Frontiers, 2022, 9, 2617-2627.	6.0	5
12	Biomass-derived porous carbon with high drug adsorption capacity undergoes enzymatic and chemical degradation. Journal of Colloid and Interface Science, 2022, 622, 87-96.	9.4	3
13	Porous Copper-Loaded Zeolites for High-Efficiency Capture of Iodine from Spent Fuel Reprocessing Off-Gas. Inorganic Chemistry, 2022, 61, 7746-7753.	4.0	23
14	Singlet oxygen-promoted one-pot synthesis of highly ordered mesoporous silica materials <i>via</i> the radical route. Green Chemistry, 2022, 24, 4778-4782.	9.0	33
15	Removal of Anionic Dyes from Aqueous Solution with Layered Cationic Aluminum Oxyhydroxide. Chemical Research in Chinese Universities, 2022, 38, 1532-1541.	2.6	1
16	Two-Dimensional Cationic Aluminoborate as a New Paradigm for Highly Selective and Efficient Cr(VI) Capture from Aqueous Solution. Jacs Au, 2022, 2, 1669-1678.	7.9	1
17	Accelerated synthesis of Al-rich zeolite beta via different radicalized seeds in the absence of organic templates. Microporous and Mesoporous Materials, 2021, 310, 110633.	4.4	9
18	Defect Engineering on Carbon-Based Catalysts for Electrocatalytic CO2 Reduction. Nano-Micro Letters, 2021, 13, 5.	27.0	118

#	Article	IF	CITATIONS
19	Reducing the dosage of the organic structure-directing agent in the crystallization of pure silica zeolite MFI (silicalite-1) for volatile organic compounds (VOCs) adsorption. Inorganic Chemistry Frontiers, 2021, 8, 3354-3362.	6.0	4
20	Enhancing catalytic performance of Cu-SSZ-13 for the NH ₃ -SCR reaction <i>via in situ</i> introduction of Fe ³⁺ with diatomite. Materials Chemistry Frontiers, 2021, 5, 7787-7795.	5.9	14
21	An efficient and stable coral-like CoFeS ₂ for wearable flexible all-solid-state asymmetric supercapacitor applications. New Journal of Chemistry, 2021, 45, 16606-16616.	2.8	8
22	The facile synthesis of core–shell PtCu nanoparticles with superior electrocatalytic activity and stability in the hydrogen evolution reaction. RSC Advances, 2021, 11, 26326-26335.	3.6	20
23	Potassium-incorporated manganese oxide enhances the activity and durability of platinum catalysts for low-temperature CO oxidation. Catalysis Science and Technology, 2021, 11, 6369-6373.	4.1	5
24	The inorganic cation-tailored "trapdoor―effect of silicoaluminophosphate zeolite for highly selective CO ₂ separation. Chemical Science, 2021, 12, 8803-8810.	7.4	32
25	Highâ€Silica CHA Zeolite Membrane with Ultraâ€High Selectivity and Irradiation Stability for Krypton/Xenon Separation. Angewandte Chemie - International Edition, 2021, 60, 9032-9037.	13.8	32
26	Highâ€Silica CHA Zeolite Membrane with Ultraâ€High Selectivity and Irradiation Stability for Krypton/Xenon Separation. Angewandte Chemie, 2021, 133, 9114-9119.	2.0	6
27	Electron Beam Irradiationâ€Induced Formation of Defectâ€Rich Zeolites under Ambient Condition within Minutes. Angewandte Chemie, 2021, 133, 14984-14989.	2.0	2
28	Electron donation of non-oxide supports boosts O2 activation on nano-platinum catalysts. Nature Communications, 2021, 12, 2741.	12.8	72
29	Electron Beam Irradiationâ€Induced Formation of Defectâ€Rich Zeolites under Ambient Condition within Minutes. Angewandte Chemie - International Edition, 2021, 60, 14858-14863.	13.8	22
30	Exsolution of Iron Oxide on LaFeO ₃ Perovskite: A Robust Heterostructured Support for Constructing Self-Adjustable Pt-Based Room-Temperature CO Oxidation Catalysts. ACS Applied Materials & Interfaces, 2021, 13, 27029-27040.	8.0	15
31	Constructing RuCoO _x /NC Nanosheets with Low Crystallinity within ZIFâ€9 as Bifunctional Catalysts for Highly Efficient Overall Water Splitting. Chemistry - an Asian Journal, 2021, 16, 2511-2519.	3.3	6
32	Photoinduced Generation of Metastable Sulfur Vacancies Enhancing the Intrinsic Hydrogen Evolution Behavior of Semiconductors. Solar Rrl, 2021, 5, 2100580.	5.8	8
33	Atomically dispersed Ni on Mo2C embedded in N, P co-doped carbon derived from polyoxometalate supramolecule for high-efficiency hydrogen evolution electrocatalysis. Applied Catalysis B: Environmental, 2021, 296, 120336.	20.2	58
34	Anionic Tuning of Zeolite Crystallization. CCS Chemistry, 2021, 3, 189-198.	7.8	20
35	Multivariate Synergistic Flexible Metalâ€Organic Frameworks with Superproton Conductivity for Direct Methanol Fuel Cells. Angewandte Chemie, 2021, 133, 26781-26785.	2.0	4
36	Multivariate Synergistic Flexible Metalâ€Organic Frameworks with Superproton Conductivity for Direct Methanol Fuel Cells. Angewandte Chemie - International Edition, 2021, 60, 26577-26581.	13.8	34

#	Article	IF	CITATIONS
37	Biâ€Functional Fe ₃ O ₄ /Au/CoFe‣DH Sandwichâ€Structured Electrocatalyst for Asymmetrical Electrolyzer with Low Operation Voltage. Small, 2021, 17, e2103307.	10.0	22
38	MoP supported on reduced graphene oxide for high performance electrochemical nitrogen reduction. Dalton Transactions, 2020, 49, 988-992.	3.3	20
39	Synthesis and properties of Mg2+ and Sr2+ coordination compounds based on in situ synthetized pyromellitdihydrazidate ligand. Journal of Molecular Structure, 2020, 1204, 127560.	3.6	3
40	β-FeOOH self-supporting electrode for efficient electrochemical anodic oxidation process. Chemosphere, 2020, 261, 127674.	8.2	15
41	Layered Inorganic Cationic Frameworks beyond Layered Double Hydroxides (LDHs): Structures and Applications. European Journal of Inorganic Chemistry, 2020, 2020, 4055-4063.	2.0	13
42	Mesoporous Nanoarchitectures for Electrochemical Energy Conversion and Storage. Advanced Materials, 2020, 32, e2004654.	21.0	109
43	A Layered Cationic Aluminum Oxyhydroxide as a Highly Efficient and Selective Trap for Heavy Metal Oxyanions. Angewandte Chemie, 2020, 132, 19707-19712.	2.0	3
44	A Layered Cationic Aluminum Oxyhydroxide as a Highly Efficient and Selective Trap for Heavy Metal Oxyanions. Angewandte Chemie - International Edition, 2020, 59, 19539-19544.	13.8	30
45	Rapid removal of Sr2+, Cs+ and UO22+ from solution with surfactant and amino acid modified zeolite Y. Microporous and Mesoporous Materials, 2020, 302, 110244.	4.4	14
46	Synthesis and Post‧ynthesis Transformation of Germanosilicate Zeolites. Angewandte Chemie, 2020, 132, 19548-19557.	2.0	4
47	Synthesis and Postâ€Synthesis Transformation of Germanosilicate Zeolites. Angewandte Chemie - International Edition, 2020, 59, 19380-19389.	13.8	48
48	Ligand substitution induced single-crystal-to-single-crystal transformations in two Ni(ii) coordination compounds displaying consequential changes in proton conductivity. Inorganic Chemistry Frontiers, 2020, 7, 1880-1891.	6.0	27
49	Synthesis, structure and photocatalytic property of a novel Zn(II) coordination polymer based on in situ synthetized pyridine-3,4-dicarboxylhydrazidate ligand. Spectrochimica Acta - Part A: Molecular and Biomolecular Spectroscopy, 2020, 233, 118232.	3.9	9
50	Highly efficient CoMoS heterostructure derived from vertically anchored Co5Mo10 polyoxometalate for electrocatalytic overall water splitting. Chemical Engineering Journal, 2020, 394, 124849.	12.7	67
51	Removal of Zn2+, Pb2+, Cd2+, and Cu2+ from aqueous solution by synthetic clinoptilolite. Microporous and Mesoporous Materials, 2019, 273, 203-211.	4.4	103
52	Pt/Al2O3 with ultralow Pt-loading catalyze toluene oxidation: Promotional synergistic effect of Pt nanoparticles and Al2O3 support. Applied Catalysis B: Environmental, 2019, 257, 117943.	20.2	101
53	Synthesis of Ni-Co Hydroxide Nanosheets Constructed Hollow Cubes for Electrochemical Glucose Determination. Sensors, 2019, 19, 2938.	3.8	31
54	Fabricating Mechanically Robust Binderâ€Free Structured Zeolites by 3D Printing Coupled with Zeolite Soldering: A Superior Configuration for CO ₂ Capture. Advanced Science, 2019, 6, 1901317.	11.2	61

#	Article	IF	CITATIONS
55	Se-incorporated Cu-based sulfide nanoparticles for enhanced hydrogen evolution. AIP Conference Proceedings, 2019, , .	0.4	Ο
56	Emerging investigator series: significantly enhanced uptake of Eu ³⁺ on a nanoporous zeolitic mineral in the presence of UO ₂ ²⁺ : insights into the impact of cation–cation interaction on the geochemical behavior of lanthanides and actinides. Environmental Science: Nano, 2019, 6, 736-746.	4.3	21
57	Condensed-matter chemistry: from materials to living organisms. National Science Review, 2019, 6, 191-194.	9.5	14
58	A chiral open-framework fluorinated cobalt phosphate consists of distorted F-encapsulated double 4-ring units with bulk homochirality. Chemical Communications, 2019, 55, 226-228.	4.1	9
59	Chiral zeolite beta: structure, synthesis, and application. Inorganic Chemistry Frontiers, 2019, 6, 1938-1951.	6.0	47
60	Stellerite-seeded facile synthesis of zeolite heulandite with exceptional aqueous Cd ²⁺ capture performance. Inorganic Chemistry Frontiers, 2019, 6, 1785-1792.	6.0	13
61	Polydopamine modified Au/FAU catalytic membrane for CO preferential oxidation. Chinese Journal of Chemical Engineering, 2019, 27, 2560-2565.	3.5	7
62	Collective excitation of plasmon-coupled Au-nanochain boosts photocatalytic hydrogen evolution of semiconductor. Nature Communications, 2019, 10, 4912.	12.8	157
63	Colloidal synthesis of high-performance FeSe/CoSe nanocomposites for electrochemical oxygen evolution reaction. Electrochimica Acta, 2019, 297, 197-205.	5.2	39
64	Synergism of Pt nanoparticles and iron oxide support for chemoselective hydrogenation of nitroarenes under mild conditions. Chinese Journal of Catalysis, 2019, 40, 214-222.	14.0	38
65	High performance proton-conducting composite based on vanadium-substituted Dawson-type heteropoly acid for proton exchange membranes. Composites Science and Technology, 2018, 162, 1-6.	7.8	40
66	A green route for the crystallization of a chiral polymorph A-enriched zeolite beta. Inorganic Chemistry Frontiers, 2018, 5, 802-805.	6.0	9
67	Unusual bulky solvent molecule encapsulation in the organic-amine-occupied 10-membered ring channels of aluminophosphate molecular sieve AlPO4-11. Inorganic Chemistry Communication, 2018, 88, 6-10.	3.9	2
68	Identification of the key factor promoting the enrichment of chiral polymorph A in zeolite beta and the synthesis of chiral polymorph A highly enriched zeolite beta. Inorganic Chemistry Frontiers, 2018, 5, 1640-1645.	6.0	12
69	Encapsulation of bulky solvent molecules into the channels of aluminophosphate molecular sieve and its negative influence on the thermal stability of open-framework. Inorganic Chemistry Communication, 2018, 91, 67-71.	3.9	3
70	Effect of degassing treatment on the deuterium permeability of Pd-Nb-Pd composite membranes during deuterium permeation. Separation and Purification Technology, 2018, 190, 136-142.	7.9	11
71	Effects of substituents on luminescent efficiency of stable triaryl methyl radicals. Physical Chemistry Chemical Physics, 2018, 20, 18657-18662.	2.8	43
72	An efficient synthetic route to accelerate zeolite synthesis <i>via</i> radicals. Inorganic Chemistry Frontiers, 2018, 5, 2106-2110.	6.0	33

#	Article	IF	CITATIONS
73	New 4-carboxylphthalhydrazidate-bridged Mn2+/In3+ coordination polymers. Journal of Molecular Structure, 2017, 1134, 728-733.	3.6	8
74	Interlayer expanded lamellar CoSe 2 on carbon paper as highly efficient and stable overall water splitting electrodes. Electrochimica Acta, 2017, 241, 106-115.	5.2	48
75	Thermoresponsive Polyoxometalate/Ionic Liquid Supramolecular Gel Electrolytes for Supercapacitors: Fabrication, Structure, and Heteropolyanion Structure Effect. Langmuir, 2017, 33, 4242-4249.	3.5	31
76	Spatial separation of the hydrogen evolution center from semiconductors using a freestanding silica-sphere-supported Pt composite. Physical Chemistry Chemical Physics, 2017, 19, 24249-24254.	2.8	5
77	Structure-directing effect on synthesis of layered aluminophosphates with same topology. Chemical Research in Chinese Universities, 2017, 33, 513-519.	2.6	4
78	Influence of fluoride ions on the structure-directing effect of organic amine in the synthesis of aluminophosphate open-frameworks. Chemical Research in Chinese Universities, 2017, 33, 853-859.	2.6	3
79	Novel Luminescent Benzimidazole-Substituent Tris(2,4,6-trichlorophenyl)methyl Radicals: Photophysics, Stability, and Highly Efficient Red-Orange Electroluminescence. Chemistry of Materials, 2017, 29, 6733-6739.	6.7	58
80	New oxalate-propagated layered Mn2+/Fe2+-4,4′-sulfoyldiphthalhydrazidate coordination polymers. Journal of Molecular Structure, 2017, 1127, 303-308.	3.6	10
81	The structure-directing effect of organic amines in the multi-template/one-structure phenomenon of microporous crystal synthesis. Microporous and Mesoporous Materials, 2017, 240, 178-188.	4.4	5
82	Phase Transition Behavior of Zeolite Y under Hydrothermal Conditions. Acta Chimica Sinica, 2017, 75, 679.	1.4	5
83	Fe ₃ O ₄ Nanoparticles Anchored on Carbon Serve the Dual Role of Catalyst and Magnetically Recoverable Entity in the Aerobic Oxidation of Alcohols. ChemCatChem, 2016, 8, 805-811.	3.7	49
84	An elaborate structure investigation of the chiral polymorph A-enriched zeolite beta. CrystEngComm, 2016, 18, 1782-1789.	2.6	19
85	Facile fabrication of thermal-control ionic liquid compound based on undecatungstophosphoindic polyoxometalate with fast ionic conductivity. New Journal of Chemistry, 2016, 40, 7923-7927.	2.8	5
86	PW9V3/rGO/SPEEK hybrid material: an excellent proton conductor. RSC Advances, 2016, 6, 84689-84693.	3.6	8
87	Temperature-dependence of the influence of the position-2-methyl group on the structure-directing effect of piperazine in the synthesis of open-framework aluminophosphates. Scientific Reports, 2016, 6, 22019.	3.3	4
88	Synthesis and high proton conductive performance of vanadium-substituted Dawson structure heteropoly acid H8P2W16V2O62·20H2O. Materials Letters, 2016, 181, 1-3.	2.6	9
89	Temperature-dependent gel-type ionic liquid compounds based on vanadium-substituted polyoxometalates with Keggin structure. Dalton Transactions, 2016, 45, 3958-3963.	3.3	18
90	Co-templated synthesis of polymorph A-enriched zeolite beta. Microporous and Mesoporous Materials, 2016, 226, 19-24.	4.4	18

#	Article	IF	CITATIONS
91	Plasmonic Au nanoparticles embedding enhances the activity and stability of CdS for photocatalytic hydrogen evolution. Chemical Communications, 2016, 52, 2394-2397.	4.1	82
92	Accelerated crystallization of zeolites via hydroxyl free radicals. Science, 2016, 351, 1188-1191.	12.6	297
93	Reversible phase transformation gel-type ionic liquid compounds based on tungstovanadosilicates. Journal of Alloys and Compounds, 2016, 660, 17-22.	5.5	9
94	Role of the FeO _x support in constructing high-performance Pt/FeO _x catalysts for low-temperature CO oxidation. Catalysis Science and Technology, 2016, 6, 1546-1554.	4.1	31
95	Origin of the structure-directing effect resulting in identical topological open-framework materials. Scientific Reports, 2015, 5, 14940.	3.3	14
96	Proton onductive membranes based on vanadium substituted heteropoly acids with <scp>K</scp> eggin structure and polymers. Journal of Applied Polymer Science, 2015, 132, .	2.6	8
97	Highly-efficient cocatalyst-free H ₂ -evolution over silica-supported CdS nanoparticle photocatalysts under visible light. Chemical Communications, 2015, 51, 10676-10679.	4.1	40
98	Thermoregulated polyoxometalate-based ionic-liquid gel electrolytes. RSC Advances, 2015, 5, 21973-21977.	3.6	19
99	Molecular engineering of microporous crystals: (VIII) The solvent-dependence of the structure-directing effect of ethylenediamine in the synthesis of open-framework aluminophosphates. Microporous and Mesoporous Materials, 2015, 208, 105-112.	4.4	13
100	Synthesis and characterization of novel azo-containing or azoxy-containing Schiff bases and their antiproliferative and cytotoxic activities. Chemical Research in Chinese Universities, 2015, 31, 60-64.	2.6	14
101	Au nanoparticle decorated N-containing polymer spheres: additive-free synthesis and remarkable catalytic behavior for reduction of 4-nitrophenol. Journal of Materials Science, 2015, 50, 1323-1332.	3.7	32
102	Influence of Al3+ on polymorph A enrichment in the crystallization of beta zeolite. Chinese Journal of Catalysis, 2015, 36, 889-896.	14.0	11
103	A dual templating route to three-dimensionally ordered mesoporous carbon nanonetworks: tuning the mesopore type for electrochemical performance optimization. Journal of Materials Chemistry A, 2015, 3, 18867-18873.	10.3	31
104	NiCo-embedded in hierarchically structured N-doped carbon nanoplates for the efficient electrochemical determination of ascorbic acid, dopamine, and uric acid. RSC Advances, 2015, 5, 65532-65539.	3.6	21
105	Synthesis of chiral polymorph A-enriched zeolite Beta with an extremely concentrated fluoride route. Scientific Reports, 2015, 5, 11521.	3.3	43
106	Facile fabrication of self-assembly polyoxometalate-type hybrid material through supermolecular interactions. Materials Letters, 2015, 154, 156-159.	2.6	7
107	Heterostructures of Ag 3 PO 4 /TiO 2 mesoporous spheres with highly efficient visible light photocatalytic activity. Journal of Colloid and Interface Science, 2015, 450, 246-253.	9.4	55
108	Rational design of carbon support to prepare ultrafine iron oxide catalysts for air oxidation of alcohols. Catalysis Science and Technology, 2015, 5, 3097-3102.	4.1	36

#	Article	IF	CITATIONS
109	Preparation and conductivity of the Keggin-type trivanadium-substituted tungstosilicic acid H7SiW9V3O40·9H2O. Materials Letters, 2014, 115, 165-167.	2.6	19
110	The structure-directing effect of n-propylamine in the crystallization of open-framework aluminophosphates. Science China Chemistry, 2014, 57, 127-134.	8.2	10
111	Correlation between the microstructures of graphite oxides and their catalytic behaviors in air oxidation of benzyl alcohol. Journal of Colloid and Interface Science, 2014, 421, 71-77.	9.4	49
112	Syntheses and electrochemical properties of polyoxometalate salts with Dawson structure. Russian Journal of Electrochemistry, 2014, 50, 398-401.	0.9	8
113	Amino-functionalized magnetic mesoporous microspheres with good adsorption properties. Materials Research Bulletin, 2014, 49, 279-284.	5.2	52
114	The temperature-dependence of the structure-directing effect of 2-methylpiperazine in the synthesis of open-framework aluminophosphates. RSC Advances, 2014, 4, 39011-39019.	3.6	9
115	Reversible phase transformation-type electrolyte based on layered shape polyoxometalate. Journal of Materials Chemistry A, 2014, 2, 5780.	10.3	53
116	A reversible phase transformation monovanadium-substituted Keggin polyoxometalate-based ionic liquid. Materials Letters, 2014, 121, 159-161.	2.6	5
117	Reversible phase transformation-type electrolyte based on Dawson-type POM and simple quaternary ammonium salt. Journal of Solid State Electrochemistry, 2014, 18, 279-283.	2.5	2
118	The dependence of the structure-directing effect of piperazine and the crystallization pathways of open-framework aluminophosphates on the local environment of the initial mixture. Microporous and Mesoporous Materials, 2014, 183, 108-116.	4.4	18
119	Preparation and Electrochemical Performance of Tungstovanadophosphoric Heteropoly Acid and Its Hybrid Materials. Journal of Physical Chemistry C, 2013, 117, 3258-3263.	3.1	64
120	A chiral open-framework fluoroaluminophosphate with enantiomeric excess in the bulk product. Chemical Communications, 2013, 49, 11287.	4.1	6
121	Molecular engineering of microporous crystals: (VII) The molar ratio dependence of the structure-directing ability of piperazine in the crystallization of four aluminophosphates with open-frameworks. Microporous and Mesoporous Materials, 2013, 176, 112-122.	4.4	18
122	Proton conducting composite materials containing heteropoly acid and matrices. Materials Chemistry and Physics, 2013, 143, 355-359.	4.0	18
123	Effect of large pore size of multifunctional mesoporous microsphere on removal of heavy metal ions. Journal of Hazardous Materials, 2013, 254-255, 157-165.	12.4	128
124	Synthesis and conductivity of hybrid materials based on germanium-containing polyoxometalates and ionic liquids. Journal of Coordination Chemistry, 2013, 66, 379-384.	2.2	9
125	Synthesis, crystal structure and conductive performance of tungstovanadophosphoric heteropoly acid H4PW11VO40·8H2O. Journal of Alloys and Compounds, 2012, 544, 37-41.	5.5	32
126	[(C4N2H12)3·H2O][(Al2P3O12)2]: A new anionic open-framework aluminophosphate with helical chains and multi-directional intersecting twelve-ring channels. Inorganic Chemistry Communication, 2012, 22, 167-169.	3.9	6

#	Article	IF	CITATIONS
127	Molecular engineering of microporous crystals: (VI) Structure-directing effect in the crystallization process of layered aluminophosphates. Microporous and Mesoporous Materials, 2012, 164, 56-66.	4.4	20
128	Molecular engineering of microporous crystals: (III) The influence of water content on the crystallization of microporous aluminophosphate AlPO4-11. Microporous and Mesoporous Materials, 2012, 147, 212-221.	4.4	47
129	Molecular engineering of microporous crystals: (V) Investigation of the structure-directing ability of piperazine in forming two layered aluminophosphates. Microporous and Mesoporous Materials, 2012, 155, 153-166.	4.4	18
130	(C4N2H12)(NH4)2[(GeO2)3(GeO1.5F3)2]: A new layered germanate containing helical arrays of H-bond. Inorganic Chemistry Communication, 2011, 14, 1842-1845.	3.9	8
131	Synthesis and conductivity of substituted heteropoly acid with Dawson structure H7[Ga(H2O)P2W17O61]·18H2O. Science Bulletin, 2011, 56, 2327-2330.	1.7	7
132	Synthesis, characterization and properties of ruthenium-substituted polyoxometallic acid H6Ru(H2O)FeW11O39·18H2O with Keggin structure. Science Bulletin, 2011, 56, 2679-2682.	1.7	4
133	Molecular engineering of microporous crystals: (II) A new method to describe the structures of zeolites and related open-framework crystalline materials. Microporous and Mesoporous Materials, 2010, 131, 148-161.	4.4	11
134	Molecular engineering of microporous crystals: (I) New insight into the formation process of open-framework aluminophosphates. Microporous and Mesoporous Materials, 2009, 123, 50-62.	4.4	24
135	Morphology Changes of Transition-Metal-Substituted Aluminophosphate Molecular Sieve AlPO4-5 Crystals. Chemistry of Materials, 2008, 20, 2160-2164.	6.7	37
136	Cotemplating Ionothermal Synthesis of a New Open-Framework Aluminophosphate with Unique Al/P Ratio of 6/7. Chemistry of Materials, 2008, 20, 4179-4181.	6.7	94
137	Synthesis, Crystal Structure, and Solid-State NMR Spectroscopy of a New Open-Framework Aluminophosphate (NH4)2Al4(PO4)4(HPO4)·H2O. Inorganic Chemistry, 2005, 44, 4391-4397.	4.0	27
138	Synthesis and characterization of a new three-dimensional aluminophosphate [Al11P12O48][C4H12N2][C4H11N2] with an Al/P ratio of 11â€â^¶â€12. Dalton Transactions RSC, 2001, , 18	30 9 -1812.	26
139	An anionic framework aluminophosphate (CH2)6N4H3·H2O [Al11P12O48] and computer simulation of the template positions. Microporous and Mesoporous Materials, 2001, 50, 151-158.	4.4	30
140	A novel open-framework aluminophosphate [AlP2O6(OH)2][H3O] containing propeller-like chiral motifs. Chemical Communications, 2000, , 1431-1432.	4.1	37
141	[Al12P13O52]3-[(CH2)6N4H3]3+:  An Anionic Aluminophosphate Molecular Sieve with Brönsted Acidity. Chemistry of Materials, 2000, 12, 2517-2519.	6.7	69
142	Structures and Templating Effect in the Formation of 2D Layered Aluminophosphates with Al3P4O163-Stoichiometry. Chemistry of Materials, 1999, 11, 2600-2606.	6.7	76
143	Anion-promoted increase of the SiO2/Al2O3 ratio of zeolites. Inorganic Chemistry Frontiers, 0, , .	6.0	6